Biochimica et Biophysica Acta 1833 (2013) 2016–2028

Contents lists available at SciVerse ScienceDirect

Biochimica et Biophysica Acta

journal homepage: www.elsevier.com/locate/bbamcr

The transcription factor NFAT1 induces apoptosis through cooperation with Ras/Raf/MEK/ERK pathway and upregulation of TNF-α expression

Bruno K. Robbs, Pedro I. Lucena, João P.B. Viola *

Program of Cellular Biology, Brazilian National Cancer Institute (INCA), Rio de Janeiro, Brazil

ARTICLE INFO

Article history:
Received 6 November 2012
Received in revised form 20 March 2013
Accepted 2 April 2013
Available online 10 April 2013

Keywords:
NFAT
Cell death
Ras
ERK
TNF-α
Tumor suppressor

ABSTRACT

Nuclear factor of activated T cells (NFAT) was described as an activation and differentiation factor in T cells. NFAT1 protein is expressed in several cell types and has been implicated in the control of the cell cycle, death and migration. Overexpression or activation of NFAT1 has been demonstrated to induce cell death in different cell types, such as T lymphocytes, Burkitt's lymphoma, and fibroblasts. Although these findings indicate a role for NFAT1 transcription factor in control of cell death, the precise mechanisms involved in this process regulated by NFAT1 are still poorly understood. The Ras/Raf/MEK/ERK pathway is activated by many growth factors and cytokines that are important in driving proliferation and preventing apoptosis and is widely implicated in cell transformation and cancer development. We show that NFAT1 protein can cooperate with Ras/Raf/MEK/ERK, but not with the JNK, p38 or NFκB pathways in cell death induction. NFAT1 can induce a cell death pathway consistent with apoptosis, which can be shifted to programmed necrosis by caspase inhibitors. Finally, through screening genes involved in cell death regulation, although we determined that TNF-α, TRAIL and PAK7 genes were up-regulated, only TNF-α expression was responsible for cell death in this context. These data suggest that NFAT1 protein activation can shift oncogenic Ras/Raf/MEK/ERK signaling to acting as a tumor suppressor pathway. These data support a potential role for regulating NFAT1 expression in gene therapy in tumors that display an activated Ras pathway, which could lead to more specific, target-directed TNF-α expression and, thus, tumor suppression.

1. Introduction

The nuclear factor of activated T cells (NFAT) family of transcription factors includes four closely related proteins, designated NFAT1-4, that are regulated by the Ca^{2+}/calcineurin pathway [1,2]. NFAT proteins have been shown to regulate the expression of a wide range of genes involved in immune system responses and vertebrate development and have more recently been implicated in cancer development [1,3,4]. An increase in intracellular calcium activates calcineurin, a calcium/calmodulin-dependent serine/threonine phosphatase, which directly dephosphorylates the NFAT regulatory domain, allowing NFAT to translocate to the nucleus and increasing its DNA affinity [5]. The immunosuppressive drugs cyclosporin A (CsA) and FK506, which are well-known inhibitors of calcineurin, inhibit NFAT activity by blocking its dephosphorylation [6]. Once located in the nucleus, NFAT proteins can bind to their target promoter elements and activate the transcription of specific responsive genes, either alone or in combination with other nuclear partners [2]. One of the main partners of NFAT activity is the synthesis and activation of the Fos and c-Jun proteins, which are components of the AP-1 family of transcription factors that can be activated by phorbol 12-muristate 13-acetate (PMA) [7].

NFAT1 is the prevalent NFAT isoform expressed in peripheral T lymphocytes. Upon T cell receptor stimulation, NFAT induces changes in the expression of a number of cytokine genes, including IL-2, IL-3, IL-4, IL-5 and IFN-γ. However, NFAT also regulates other responsive genes, such as c-myc, $p21^{Waf1}$, CD40 ligand, FasL, CDK4 and Nur77, indicating that these transcription factors may also be involved in the control of the cell cycle and apoptosis [8–10]. Indeed, three-month-old NFAT1 deficient ($NFAT1^{-/-}$) mice develop a lymphocyte hyperproliferative phenotype, reflected by a slight size increase in peripheral lymphoid organs, accompanied by a reduction in cell death and an increased cell cycle rate [11–14]. $NFAT1^{-/-}$ mice also exhibit neoplastic transformation of cartilage cells, which resemble chondrosarcomas and display an increased propensity for chemical carcinogen-induced tumor formation [15,16].

The phenotype of NFAT1-deficient mice suggests that this family of transcription factors is likely to play a much broader role in the regulation of cell death than previously described and might be involved in tumorigenesis. Overexpression or activation of NFAT1 protein has been demonstrated to induce cell death in different cell types, such as T lymphocytes, Burkitt's lymphomas, and fibroblasts [16–20]. Recently, our group demonstrated that NFAT1 protein can induce cell

* Corresponding author at: Programa de Biologia Celular, Instituto Nacional de Câncer (INCA), Rua André Cavalcanti, 37, Centro, Rio de Janeiro, RJ 20231-050, Brazil. Tel.: +55 21 3207 6530; fax: +55 21 3207 6587.
E-mail address: jpviola@inca.gov.br (J.P.B. Viola).

0167-4889/$ – see front matter © 2013 Elsevier B.V. All rights reserved.
http://dx.doi.org/10.1016/j.bbamcr.2013.04.003

death in NIH3T3 fibroblasts transformed with the H-*rasV12* oncogene and can act as a tumor suppressor gene that reduces tumor formation in mice [16]. Although these data propose a role for the NFAT1 transcription factor in the control of cell death, the precise genetic mechanisms involved in this process regulated by NFAT1 are still poorly described.

The Ras/Raf/MEK/ERK pathway is activated by many growth factors and cytokines that are important in driving proliferation and preventing apoptosis [21–23]. This signaling pathway is found to be mutationally activated or overexpressed in several human cancers, such as melanomas, colorectal, pancreatic, papillary-thyroid and serous ovarian carcinomas and lung cancers [24–28]. Furthermore, studies using genetic or pharmacologic approaches have shown that MEK (MAPK/ERK kinase) and ERK (extracellular signal-regulated kinase) protein activities are required for the transforming activities of Ras [29], thus supporting an oncogenic role for this pathway.

In this study, we aimed to determine the signaling pathways that can cooperate with NFAT1, the mechanism of cell death, and the critical genes that are regulated by NFAT1 protein in the induction of cell death. We show that the activation of NFAT1 can induce cell death in NIH3T3 fibroblasts only in cooperation with the oncogenic Ras pathway. Furthermore, NFAT1 cooperates with the Ras/Raf/MEK/ERK pathway in the induction of cell death, but not with other pathways downstream of Ras, such as the JNK (c-Jun N-terminal kinase) or p38 kinase pathway. NFAT1 induces a cell death phenotype characterized as apoptosis that can be shifted to programmed necrosis in the presence of caspase inhibitors. Finally, a PCR array analysis of genes involved in apoptosis showed that TNF-α (tumor necrosis factor alpha) presented the most abundant mRNA up-regulation in response to NFAT1 activation, leading to massive TNF-α protein production that was directly implicated in the induction of cell death. Collectively, these data suggest that NFAT1 protein can induce cell death through the regulation of TNF-α expression and that this phenotype is dependent on the activation of the Ras/Raf/MEK/ERK pathway.

2. Experimental procedures

2.1. Cell culture and reagents

NIH3T3 cell cultures were maintained in Dulbecco's modified Eagle's medium (DMEM) supplemented with 10% fetal bovine serum (FBS). Cells were cultured in a humidified environment containing 5% CO_2 at 37 °C. Inhibitors of p38 kinase (SB-203580), MEK1/2 (U0126 and PD98059) and JNK (SP600125) were all purchased from ENZO Life Science, while 4-hydroxytamoxifen (OHT) was obtained from Invitrogen. Phorbol 12-muristate 13-acetate (PMA) was obtained from Calbiochem. Recombinant mouse TNF-α (T7539) was acquired from Sigma. Phycoerythrin-conjugated Annexin-V, 7-AAD, and Ac-DEVD-AFC were obtained from BD Biosciences. Pan and Caspase-3 inhibitors (Z-VAD-FMK and Z-DEVD-FMK respectively), and necrostatin-1 were obtained from R&D Systems. The NFAT1 polyclonal antibody anti-67.1 was a gift from Dr. Anjana Rao [30]. GAPDH (6C5) and pan-Ras (sc-32) were obtained from Santa Cruz Biotechnology; total- (#9102) and phospho-ERK1/2 (#9106) were obtained from Cell Signaling, and a TNF-α neutralizing antibody (MCA1488XZ) was obtained from AbD Serotec.

2.2. Plasmid constructs

CA-NFAT1 murine cDNA has previously been described [31] and was a gift from Dr. Anjana Rao. The plasmid pLIRES-EGFP-CA-NFAT1 was constructed by subcloning CA-NFAT1 cDNA into the pLIRES-EGFP backbone retroviral plasmid [32]. To construct a plasmid containing NFAT1 protein responsive to the synthetic steroid 4-hydroxytamoxifen (OHT), designated pLIRES-EGFP-CA-NFAT1-ER, a Sal1 restriction site was introduced immediately after the CA-NFAT1 C-terminus at the original stop codon using the GeneTailor Site-Directed Mutagenesis system (Invitrogen). The original CA-NFAT1 construct contains an SV40 nuclear localization signal (NLS) at its C-terminus adjacent to its stop codon; in pLIRES-EGFP-CA-NFAT1-ER, the NLS was excluded. The N-terminally truncated G525R estrogen receptor responsive to tamoxifen (ER™) was PCR amplified from pBabe-*c-myc*ER™, a gift from Dr. Gerard Evan, and subcloned at the Sal1 site to create pLIRES-EGFP-CA-NFAT1-ER [33]. The retroviral plasmids pBabe-H-*ras*V12, pBabe-IκBα-mut (Addgene plasmid 15291) and pBabe-MEK1^{DD} (Addgene plasmid 15268) were described previously [34,35] and were a gift from Dr. Scott Lowe or acquired from Addgene. The luciferase reporter construct 3×NFAT-Luc (pGL4.30; Promega), which contains three copies of the distal NFAT-AP1 site of the IL-2 promoter [36], and 6×NFκB, containing six copies of the NFκB responsive element [37], were constructed as described previously. All constructs were confirmed by restriction enzyme mapping and DNA sequencing.

2.3. Production of recombinant retroviruses and infection of NIH3T3 cells

The BD EcoPack2 ecotropic packaging cell line (BD-Biosciences) was transiently transfected with a retroviral vector via calcium phosphate precipitation for 24 h. Cell-free virus-containing supernatant was collected 48 h after transfection, mixed 1:1 with fresh medium, supplemented with 8 μg/ml polybrene (FLUKA Chemie, Buchs, Switzerland), and immediately used for spin-infection (2 × 45 min at 420 g, room temperature) of 2.5×10^4 NIH3T3 cells. Infected cells were incubated at 37 °C for an additional 24 h, trypsinized, and used as indicated. To ensure reproducibility, each experiment was repeated using cells derived from independent viral infections.

2.4. NIH3T3 cells expressing CA-NFAT1-ER, H-rasV12, MEK1^{DD} and IκBα-mut construction

NIH3T3-CA-NFAT1-ER or -Empty-Vector cells were generated by transducing NIH3T3 wild-type cells with the pLIRES-EGFP-CA-NFAT1-ER retroviral vector or Empty Vector following selection for G418 (Invitrogen) resistance (1000 μg/ml) for 14 days. NIH3T3-CA-NFAT1-ER cells expressing H-*ras*V12, MEK1^{DD} or IκBα-mut were generated by transducing the cells with the pBabe-H-*ras*V12, -MEK1^{DD} or -IκBα-mut retroviral vector following selection for puromycin (Sigma) resistance (15 μg/ml) for at least 5 days.

2.5. Cell proliferation studies

NIH3T3-Empty-Vector or -CA-NFAT1-ER cells infected with H-rasV12 when indicated were plated in triplicate into 96-well microtiter plates at a density of 8×10^3 cells per well and treated with 100 nM OHT and 20 nM PMA. When indicated, the cells were pre-treated with U0126 2 h prior to OHT addition. Cell proliferation was analyzed at the indicated times by a Crystal Violet assay, which involves fixing the cells with ethanol for 10 min, followed by staining with 0.05% Crystal Violet in 20% ethanol for 10 min and solubilization with methanol. The plate was read on a spectrometer at 595 nm.

2.6. Sub-G_0 and cell permeabilization analyses

Twelve microtiter plates were inoculated with 1×10^5 cells and treated with OHT (100 nM) and PMA (20 nM) or with mouse recombinant TNF-α as indicated. When indicated, the cells were treated with SB-203580 (1 to 80 μM), U0126 (1–80 μM), SP600125 (20–100 μM), Z-VAD-FMK (20 μM), necrostatin-1 (20 μM) or the TNF-α neutralizing antibody (0.5 to 4 μg/ml) 2 h prior to OHT or TNF-α addition. On the indicated day, the cells were trypsinized, and the supernatant was collected and washed once with phosphate-buffered saline (PBS). Cells were then stained with propidium iodide (75 μM) in the presence of NP-40 for Sub-G_0 analysis, or with saline

PBS with propidium iodide (5 μg/ml) for permeabilization analysis. Analyses of DNA content and PI-positive cells were conducted by collecting 20,000 events using a FACScalibur flow cytometer and CELLQuest software (BD Biosciences).

2.7. Annexin-V staining

NIH3T3-CA-NFAT1-ER cells were plated at a density of 1.5×10^6 cells/10 cm dish and treated with OHT (100 nM) and PMA (20 nM) when indicated. At different time-points, the cells were trypsinized, and the supernatant was collected, washed with PBS, stained with Annexin V-PE and 7-AAD, and analyzed by flow cytometry.

2.8. Transactivation assay

NIH3T3-CA-NFAT1-ER cells infected with pBabe-Empty or pBabe-IκBα-mut when indicated were plated at 2.5×10^5 cells/10 cm dish. After 24 h, the cells were cotransfected via calcium phosphate precipitation with the 3×NFAT-Luc (10 μg) or the 6xNFκB-Luc (10 μg) reporter plasmid and a *Renilla* luciferase expression plasmid (pRL-TK) for normalization (1 μg). After 24 h, the cells were trypsinized, and 1×10^5 cells were plated in a 24-well plate, followed by the addition of OHT (100 nM) or PMA (20 nM) 2 h later. At the indicated times, cells were harvested and lysed with 40 μl of lysis reagent (Promega). Crude extracts were analyzed in a Veritas microplate luminometer (Turner Biosystems) using a dual-luciferase reporter assay system (Promega) as directed by the manufacturer. The firefly luciferase reporter gene was normalized with the *Renilla* vector pRL-TK. Luciferase activities were expressed as relative light units (RLU).

2.9. Western blotting

NIH3T3 cells infected with Empty Vector or NFAT1 WT, CA-NFAT1, CA-NFAT1-ER, H-rasV12 or $MEK1^{DD}$ were treated when indicated with OHT (100 nM), PMA (20 nM) or U0126 (1–20 μM). Total protein was obtained from 3.5×10^5 cells by cell lysis in buffer containing 40 mM Tris pH 7.5, 60 mM sodium pyrophosphate, 10 mM EDTA, and 5% SDS, followed by incubation at 100 °C for 15 min. Total cell lysates were resolved via SDS-PAGE, and the proteins were transferred to a nitrocellulose membrane. Antibodies against pan-Ras, NFAT1, total- and phospho-ERK, and GAPD were used as indicated in the Cell culture and reagents section and in the figure legends. Immunodetection was performed with an ECL Western blotting detection kit (GE Healthcare).

2.10. NFAT immunolocalization and pyknotic nuclei analyses

NIH3T3-CA-NFAT1-ER cells were treated with OHT (100 nM) and PMA (20 nM) when indicated and fixed in 4% paraformaldehyde at room temperature for 15 min. The cells were permeabilized, and nonspecific sites were blocked with 1× PBS containing 0.5% NP-40 and 5% FBS in several 5 min washes. For NFAT1 immunolocalization, cells were incubated for 1 h at room temperature with an NFAT1 polyclonal antibody in 1× PBS containing 0.5% NP-40 and 5% FBS. Then, the cells were washed again prior to incubation with rhodamine-labeled anti-rabbit IgG (KPL) for 30 min. For nuclear staining and to examine the formation of pyknotic nuclei, the cells were incubated with DAPI (300 nM) for 1 min. The cells were viewed under an Olympus FluoView FV10i confocal fluorescence microscope. NFAT1 subcellular localization was quantified by counting at least 100 randomly chosen DAPI stained cells and determination of NFAT1 localization.

2.11. ELISA against TNF-α

NIH3T3-CA-NFAT1-ER cells or cells expressing Empty Vector, H-rasV12 or $MEK1^{DD}$ were treated with OHT (100 nM) and PMA (20 nM) as indicated. When indicated, cells were treated with U0126 (20 μM) 2 h prior to OHT and PMA. At different time-points, cell-free supernatant was assessed for TNF-α protein levels using the Murine TNF-α ELISA Development kit (PeproTech) according to the manufacturer's instructions.

2.12. Enzymatic assay for caspase-3 activity

Caspase-3 activity was measured using the fluorogenic enzyme substrate Ac-DEVD-AFC. Cells were plated (1.5×10^6 cells/10 cm plate) and treated with OHT (100 nM) and PMA (20 nM) as indicated. After 24 h, the cells were collected as a pellet and resuspended in 50 μl of cell lysis buffer, then incubated on ice for 30 min. The cells were then centrifuged at 3000 *g* for 5 min, and the supernatant was transferred to a 96-well plate, to which 50 μl of reaction buffer (20 mM PIPES, pH 7.4, 1 mM EDTA, 0.1% CHAPS, 10% Sucrose, 10 mM DTT, 100 mM $NaCl_2$) containing 10 μg/ml of the substrate was added. As a control, the caspase-3 inhibitor Ac-DEVD-FMK (10 μg/ml) was added when indicated. The plate was incubated at 37 °C for 1 h, and the samples were read in a fluorometer equipped with a 400 nm excitation filter and a 505 nm emission filter or in a spectrum with emissions varying between 480 and 520 nm. The protein content was measured using Bradford Folin's reagent method (Bio-Rad Laboratories) and used to normalize enzyme activity, which was expressed as a % relative to cells treated with PMA alone.

2.13. Real-time reverse transcriptase (SYBR Green) SuperArray assay

NIH3T3-CA-NFAT1-ER cells were treated with OHT (100 nM) and PMA (20 nM) as indicated for 24 h, and total mRNA was isolated from cells using RNeasy Mini Spin Columns (Qiagen), according to the manufacturer's protocol. The purity and quantity of total RNA were determined using a Nanodrop UV–visible spectrophotometer (Nano-Drop Technologies), and RNA integrity was assessed based on the 28S and 18S ribosomal mRNA bands via agarose gel electrophoresis. First-strand DNA was synthesized using the RT2 First Strand kit (SABiosciences Corporation) as recommended by the manufacturer. Real-time polymerase chain reaction (RT-PCR) was performed using STBR Green PCR Master Mix (SABiosciences) in a 7500 Fast Real-Time PCR System (Applied Biosciences) according to the manufacturer's instructions. The quality of the primers was tested via the analysis of the melting curve. We used the PAMM-012 Mouse Apoptosis Pathway RT Profiler PCR array (SABiosciences), which profiles the expression of 84 genes involved in apoptosis-related signaling.

3. Results

3.1. Both NFAT1 activation and PMA stimulation are required for the induction of cell death in fibroblasts

Although several recent studies suggest that NFAT1 protein can induce cell death when overexpressed or activated in different cell types, the precise cell death machinery involved in this process is still not well characterized [16–20]. To address this question, we constructed a conditional NFAT1 protein responsive to the synthetic steroid 4-hydroxytamoxifen (OHT) by fusing the previously characterized constitutively active NFAT1 protein (CA-NFAT1) [16,31] to the N-terminally truncated G525R estrogen receptor (ER™), which is only responsive to OHT (CA-NFAT1-ER; Fig. 1A) [33]. CA-NFAT1-ER cDNA was cloned into the retroviral vector pLIRES-EGFP, which was then used to transduce NIH3T3 cells, and these cells were subsequently stabilized via antibiotic resistance (NIH3T3-CA-NFAT1-ER cells). The use of a conditioned

NFAT1 protein allows temporal control and synchronization of NFAT activation and, thus, a more detailed analysis of [1] the pathways that can cooperate with NFAT [2], the gene expression profile mediated by this factor [3], and cell death kinetics. Furthermore, this construct bypasses the need for a Ca^{2+} influx to activate NFAT1 protein and therefore allows the reduction of the background generated by the induction of other Ca^{2+}-responsive transcription factors, such as CREB and MEF2 [38–40]. Subsequent expression analysis in NIH3T3-CA-NFAT1-ER cells of the encoded CA-NFAT1-ER construct demonstrated that the protein functioned properly and exhibited all of the expected characteristics. The CA-NFAT1-ER protein presented the expected apparent molecular weight compared to wild-type or constitutively active NFAT1 protein (Fig. 1B), was restricted to the cytoplasm (>95% of total cells) and completely translocated to the nucleus (>95% of total cells) when treated with OHT (Fig. 1C), and showed the ability to transactivate an NFAT-responsive reporter luciferase construct (pGL4.30) in a time-dependent manner, reaching a plateau in 24 h, only in the presence of OHT (Fig. 1D).

Next, we analyzed the role of the NFAT1 protein in the control of cell proliferation and death (Fig. 2). The growth capacity of NIH3T3 cells expressing CA-NFAT1-ER was assessed in a proliferation kinetics assay, accompanied by crystal violet incorporation, which correlates with total cell numbers, while cell death kinetics were accompanied by sub-G_0 DNA content, which is indicative of cells undergoing apoptosis. There was no difference between empty vector- and CA-NFAT1-ER-expressing cells in their proliferation (Fig. 2A) and apoptosis profiles (Fig. 2B), with the activation of the CA-NFAT1-ER protein observed only following OHT application. However, the addition of the phorbol 12-muristate 13-acetate (PMA) induced a strong decrease in cell accumulation rate (Fig. 2C) accompanied by cell death (Fig. 2D) only in cells expressing and showing activated CA-NFAT1-ER following treatment with OHT. The profile of cells undergoing cell death exhibiting a sub-G_0 DNA content can be further visualized from the results of the two representative flow cytometric analysis (Fig. 2E and F). Furthermore, NIH3T3 cells showing activated CA-NFAT1-ER in the presence of PMA displayed time-dependent cell death induction, culminating with massive cell death at 72 h after NFAT1 activation (Fig. 2D). Altogether, these data demonstrate that while OHT and PMA do not alter proliferation and death in empty vector-expressing cells, they do induce a strong cell death phenotype in NIH3T3-CA-NFAT1-ER cells, supporting the idea that cell death is caused by NFAT1 activation and that it depends on cooperation with a pathway activated downstream of PMA.

3.2. NFAT1 cooperates with the oncogenic Ras/Raf/MEK/ERK pathway in the induction of cell death, but not with the NFκB pathway

To further investigate the pathways that can cooperate with NFAT1 in the induction of cell death, we analyzed the two main downstream PMA-activated pathways: the NFkB and Ras/MAPK (mitogen-activated protein kinase) pathways. To examine whether the NFκB transcription factor can cooperate with NFAT1 in the induction of cell death in fibroblasts, NIH3T3-CA-NFAT1-ER cells were transduced with an empty vector or with a plasmid encoding a dominant-negative mutated IκBα (IκBα-Mut) protein [35]. As expected, NIH3T3-CA-NFAT1-ER cells carrying the empty vector underwent cell death 72 h after treatment with OHT and PMA (Fig. 3A). However, the inhibition of NFκB activation via overexpression of IκBα-Mut did not prevent the induction of cell death by NFAT1 activation in cells treated with OHT and PMA (Fig. 3A). The dominant-negative IκBα protein was functioning properly, as it was able to completely block PMA induction of NFκB transactivation of an NFκB-responsive luciferase promoter (Fig. 3B). These data support the idea that the NFκB signaling pathway is not essential for NFAT1 induction of cell death.

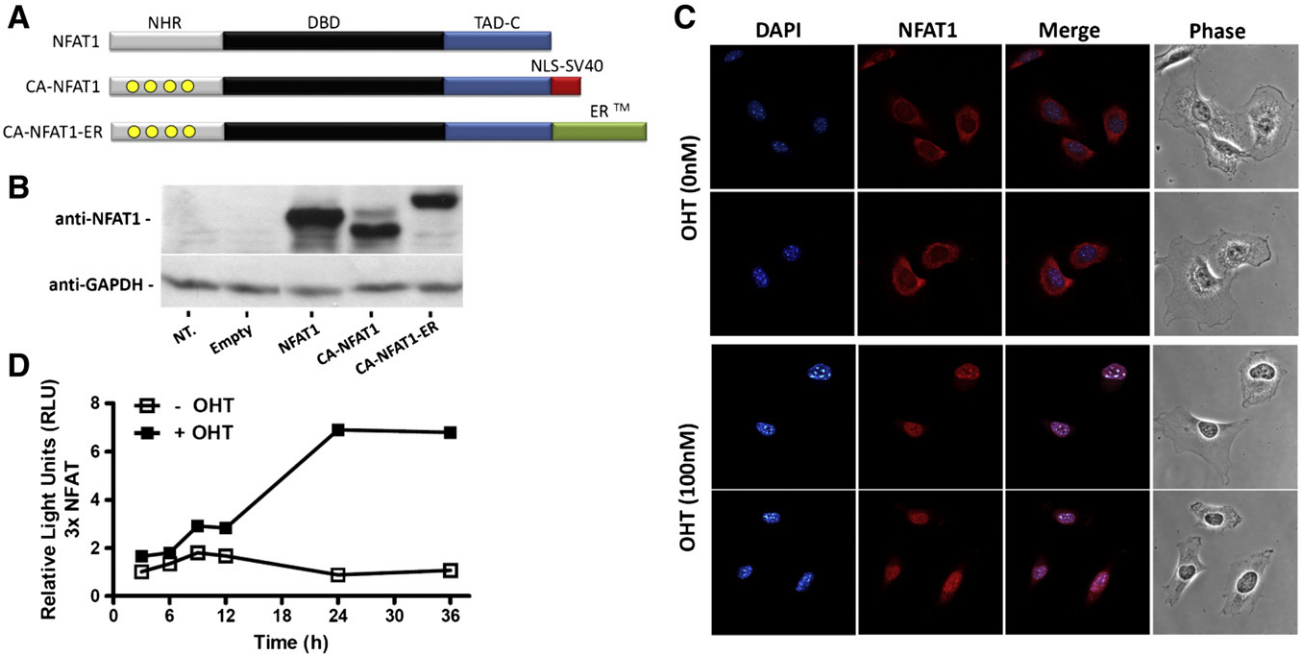

Fig. 1. Construction and validation of 4-hydroxytamoxifen responsive NFAT1 protein (CA-NFAT1-ER). A) Schematic alignment of the NFAT1 protein and constructs. Abbreviations and schematic conventions: serine to alanine CA-NFAT1 mutations (yellow circles), DNA-binding domain (DBD, dark bars), C-terminal transactivation domains (TAD-C, blue bars), NFAT homology region (NHR, gray bars), nuclear localization signal from the SV40 virus (NLS-SV40, red bar) and N-terminally truncated G525R estrogen receptor (ER™, green bar). Identical shading patterns represent identical sequences. CA-NFAT1-ER was constructed by deleting the NLS-SV40 signal from the CA-NFAT1 protein, followed by fusion with the truncated estrogen receptor responsive to 4-hydroxytamoxifen (OHT), as described. B) NFAT1 protein expression determined by western blotting analysis of NIH3T3 cells retrovirally transduced with the indicated construct. GAPDH levels were used as a loading control. Non-transduced cells (ND). C) The subcellular localization of NFAT1 protein in NIH3T3-CA-NFAT1-ER cells was determined by fluorescence microscopy in the presence of 0 or 100 nM OHT for 24 h. Cells were stained with DAPI and anti-NFAT1-PE Abs. and visualized by fluorescence and phase contrast microscopy. D) NFAT transactivation assay. NIH3T3-CA-NFAT1-ER cells were transfected with pGL4.30 (NFAT responsive vector) and pRL-TK (*Renilla* normalization vector). After 24 h, they were treated with OHT (100 nM) when indicated. Luciferase activity was measured as described at the specified times and was expressed as light units relative to the first time point in cells without OHT. All results are representative of at least 3 independent experiments.

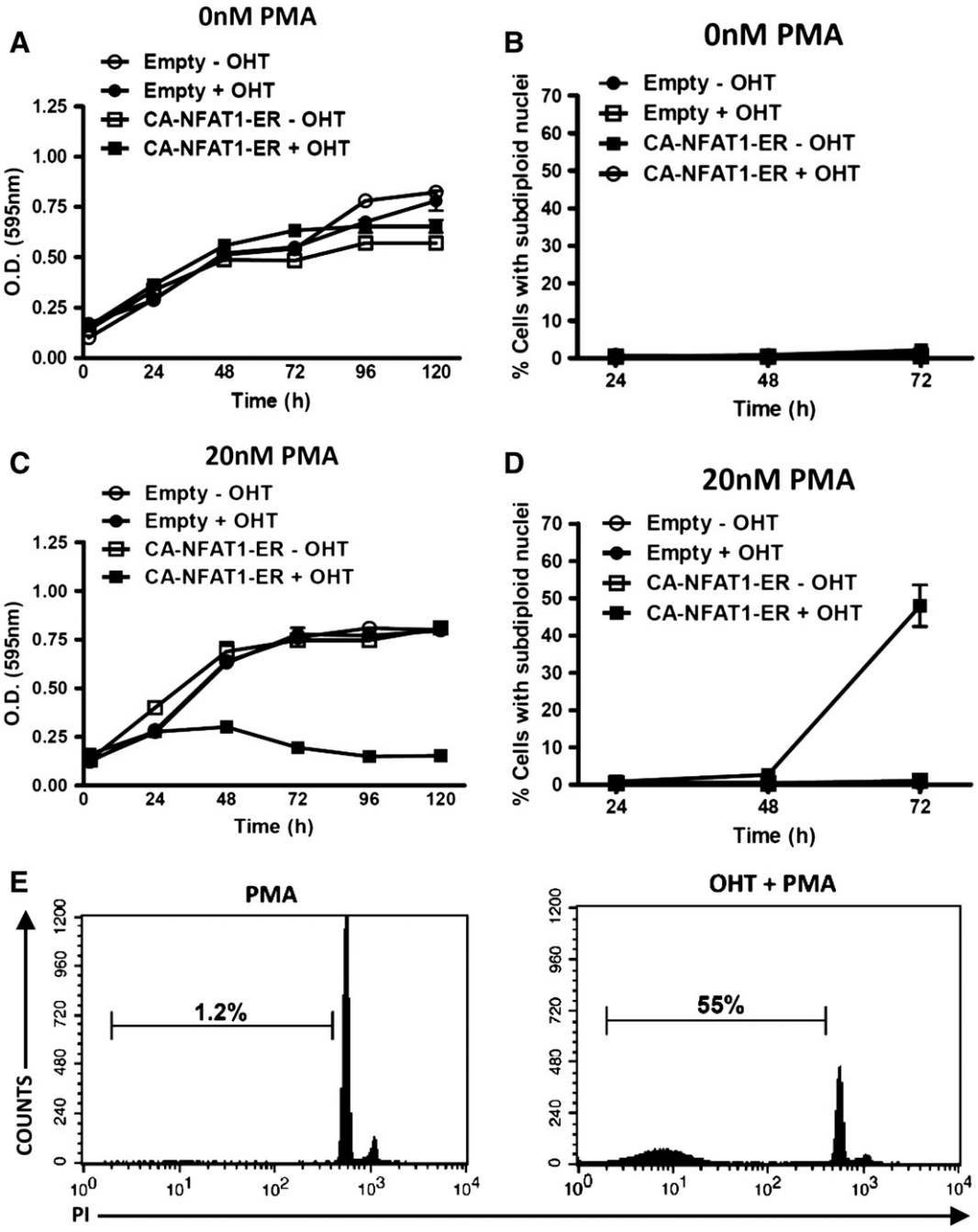

Fig. 2. NFAT1 induces cell death and reduces proliferation only in cooperation with a PMA-activated pathway. NIH3T3-Empty-Vector or -CA-NFAT1-ER cells were plated and analyzed for cell growth and death as indicated below. A and C) Analysis of proliferation kinetics based on Crystal Violet staining. Cells were plated in the absence (A) or presence (C) of 20 nM phorbol 12-muristate 13-acetate (PMA) and in the presence of OHT (100 nM) when specified. The results are representative of at least 3 independent experiments. B and D) Cell death analysis based on the formation of subdiploid nuclei (Sub-G_0). Cells were plated in the absence (B) or presence (D) of 20 nM PMA and in the presence of OHT (100 nM) when indicated. Cells were stained with PI and analyzed by flow cytometry to determine their DNA content at the specified time. SD values indicate the variance of at least three independent experiments. E) Representative Sub-G_0 cell death analysis histograms from NIH3T3-CA-NFAT1-ER cells treated with PMA (20 nM) (left panel) and OHT (100 nM) (right panel) for 72 h, extracted from Fig. 2D. The percentage of cell death (Sub-G_0) is indicated.

Stimulation of cells with PMA is also known to activate the Ras/MAPK pathway directly through the activation of RasGRPs (Ras guanyl nucleotide-releasing proteins) or indirectly through the activation of PKC protein [41,42]. To investigate whether the Ras/MAPK pathway is involved in the induction of cell death by NFAT1, NIH3T3-CA-NFAT1-ER-expressing cells were transduced with an empty vector or with a plasmid encoding the constitutively active H-*ras*V12 protein. H-*ras* protein expression was analyzed by western blotting to confirm the overexpression of this oncogene (Fig. 3C). As expected, only low levels of cell death were visualized when assessed at an early time point, 48 h after treatment with OHT and PMA, in the NIH3T3-CA-NFAT1-ER plus empty-vector-expressing cells (Fig. 3D). However, the activation of NFAT1 protein by OHT treatment in NIH3T3-CA-NFAT1-ER cells expressing the H-*ras*V12 oncogene was sufficient to induce massive cell death at this time point (Fig. 3D; OHT). These data suggest that H-*ras*V12 expression can induce cell death in cooperation with NFAT1 at an earlier time point (48 h) when compared to cells treated only with OHT and PMA (72 h; Fig. 2D). The H-*ras*V12 overexpression may accelerate the cell death induced by NFAT1 when compared with PMA stimulation. In fact, this phenotype can be readily visualized at cell proliferation analysis

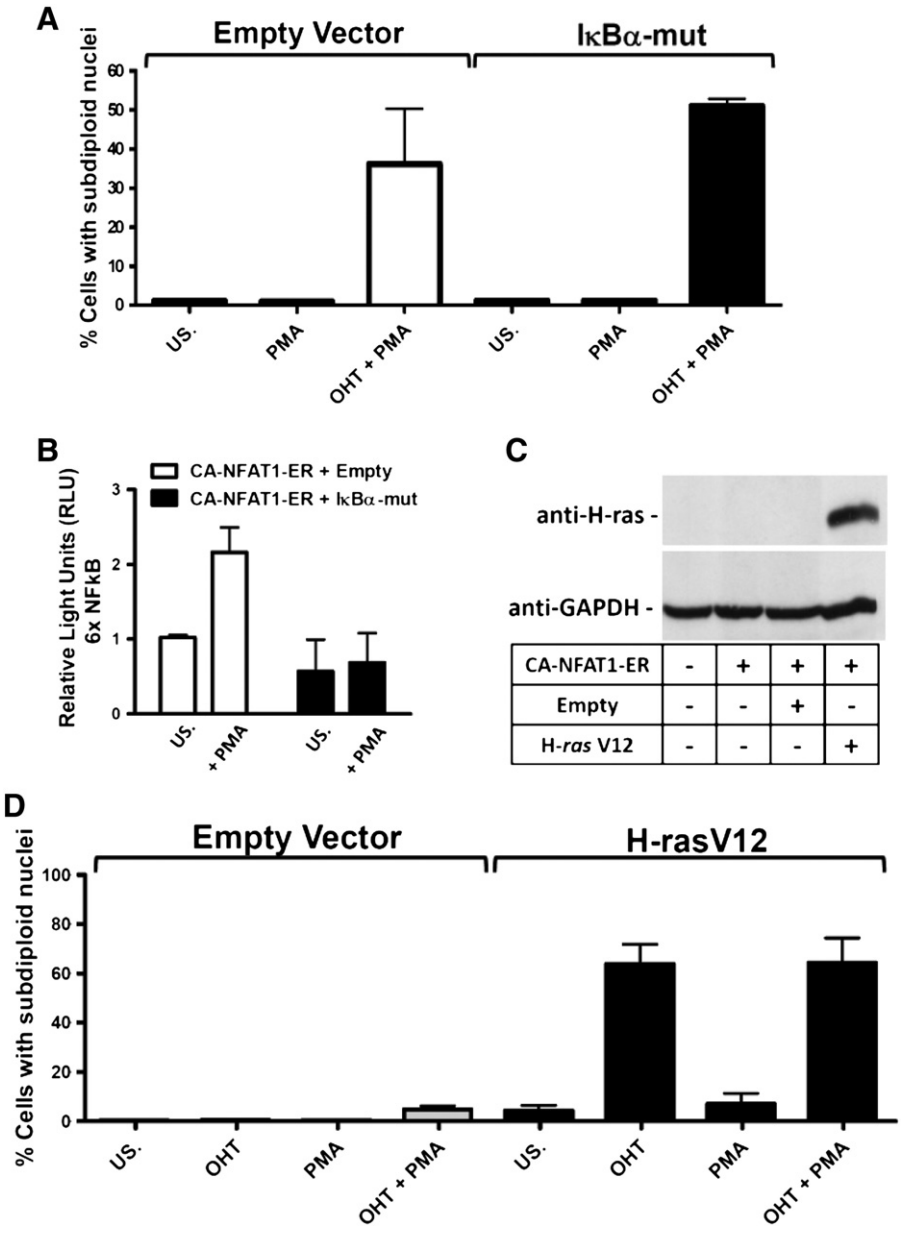

Fig. 3. The H-*ras*, but not the NFκB pathway cooperates with the induction of cell death by NFAT1. A and D) Cell death analysis based on the formation of subdiploid nuclei (Sub-G_0). NIH3T3-CA-NFAT1-ER cells were transduced with the indicated vector (pBabe-Empty; -IkBα-mut or -H-*ras*V12) as described. Cells were plated, treated with OHT (100 nM) and PMA (20 nM) as specified and cultured for 72 h (A) or 48 h (D). Cells were stained with PI and analyzed by flow cytometry for DNA content. B) NFκB transactivation assay. NIH3T3-CA-NFAT1-ER-expressing cells were transduced with the Empty or IκBα-mut construct as described. Then, the cells were transfected with pGL3-6×NFκB (NFκB responsive vector) and pRL-TK (*Renilla* normalization vector). On the next day, the cells were treated with PMA (20 nM) for 6 h. Luciferase activity was measured as described and was expressed as relative light units (RLU) compared to the first graphic column. SD values indicate the variance of three independent experiments. C) H-*ras*V12 protein expression. Western blotting analysis of NIH3T3 cells retrovirally transduced with the indicated plasmids for H-ras protein expression. GAPDH levels were used as a loading control. The results are representative of at least 3 independent experiments. US. denotes unstimulated cells in all experiments.

comparing Figs. 2C and 4H. Furthermore, stimulation with PMA did not result in a cooperative effect to further increase cell death in cells expressing H-*ras*V12 treated with OHT (Fig. 3D; OHT + PMA). Altogether, these data demonstrate that H-*ras*V12 overexpression is sufficient to bypass the need for PMA in the induction of cell death by NFAT1, supporting the idea that NFAT1 can cooperate with pathways downstream of Ras/MAPK.

Activation of Ras protein through the induction of a phosphorylation cascade involving several downstream MAPKKK pathways culminates the induction of three main families of MAPKs, ERK1/2, JNK1/2/3, and p38α/β/γ/δ kinases [29,43]. However, the JNK and p38 pathways appear not to be involved in the induction of cell death by NFAT1 because the use of JNK- and p38-specific inhibitors (SP600125 and SB203580) to produce a dose-response curve, at concentrations ranging from 1 μM up to 80 μM, did not inhibit the induction of cell death by NFAT1 (Fig. 4A). On the other hand, the Ras/Raf/MEK/ERK pathway appears to be fundamental for the induction of cell death by NFAT1 (Fig. 4B–H). MEK1/2 is the MAPKK upstream of ERK1/2, and their inhibition by the drug U0126 is used to evaluate ERK-mediated events. To examine whether the Ras/Raf/MEK/ERK pathway is involved in the induction of cell death by NFAT1, NIH3T3-CA-NFAT1-ER cells were transduced with H-*ras*V12 and treated with U0126 to obtain a dose-response curve (Fig. 4B). MEK1/2 inhibition led to a reduction of the cell death induced by NFAT1 activation (OHT) in a concentration-dependent manner in which inhibition with U0126 at 5 μM was sufficient to reduce total cell death by 50% and 20 μM by approximately 90% (Fig. 4B). Inhibition of MEK1/2 by U0126 was correlated with the reduction of ERK1/2

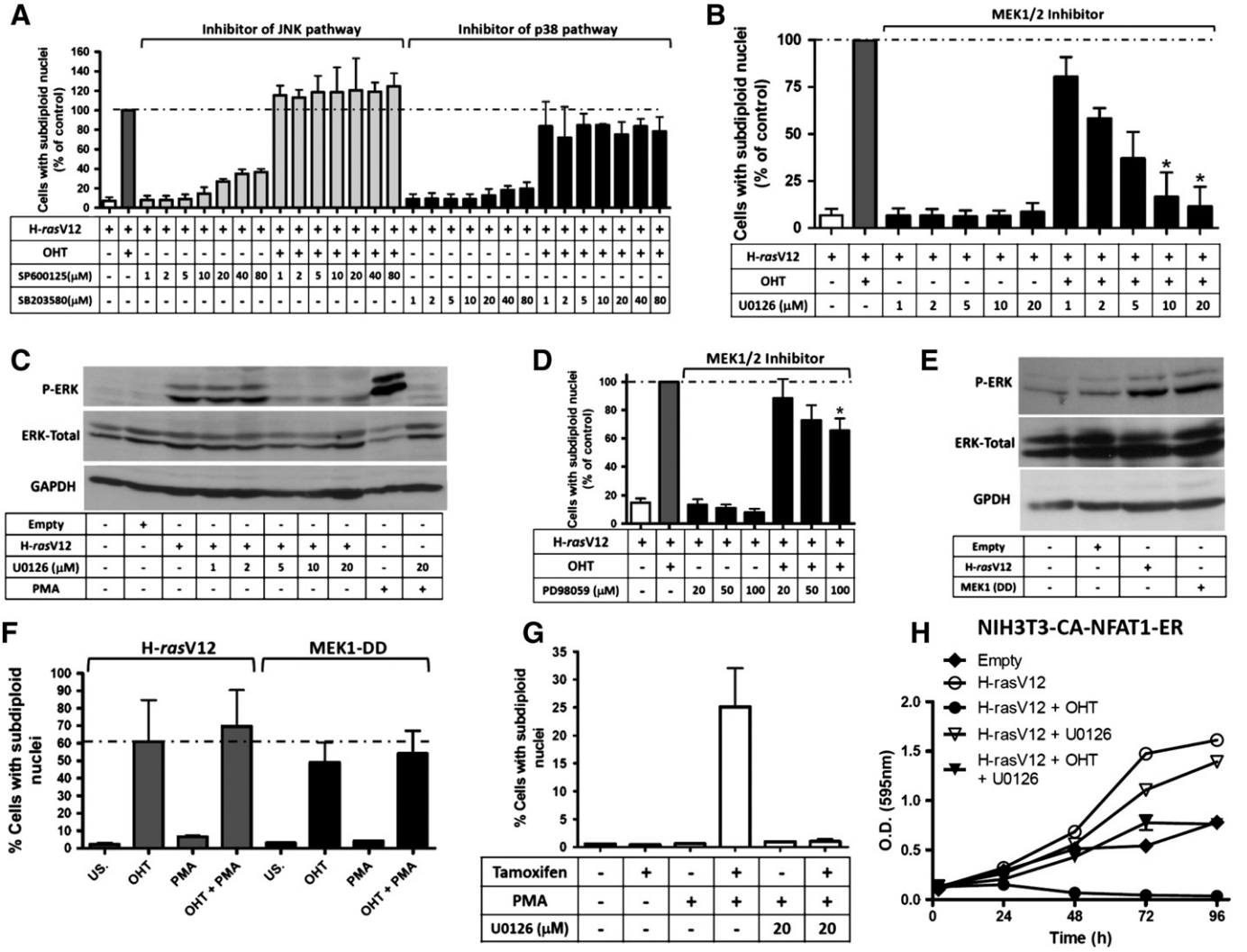

Fig. 4. The Ras/Raf/MEK/ERK pathway, but not p38 or JNK cooperates with the induction of cell death by NFAT1. A, B, D, F and G) Cell death analysis based on the formation of subdiploid nuclei (Sub-G_0). NIH3T3-CA-NFAT1-ER cells were transduced with the indicated vectors (pBabe-H-*ras*V12; MEK1-DD) as described. When specified, cells were pre-treated with variable concentrations of SP600125 (JNK inhibitor), SB203580 (p38 inhibitor), U0126 or PD98059 (MEK1/2 inhibitors) 2 h prior to stimulation. Cells were treated with OHT (100 nM) and PMA (20 nM) when indicated and cultured for 48 h (A, B, D and F) or 72 h (G) before being stained with PI and analyzed by flow cytometry to determine their DNA content. SD values indicate the variance of at least three independent experiments, and (*) indicates $p \leq 0.001$. C and E) Western blotting analysis of the ERK1/2 phosphorylation state. NIH3T3-CA-NFAT1-ER cells were retrovirally transduced with the specified plasmid (pBabe-Empty; -H-*ras*V12 or -MEK1^{DD}) as described. When indicated, cells were pre-treated for 2 h with variable concentrations of U0126 prior to the addition of PMA (20 nM). The cells were harvested and analyzed as described 24 h after PMA stimulation. GAPDH and total-ERK were used as loading controls. C) The two last lanes of the gel suffered an upshift that can be seen in all conditions (p-ERK; ERK-Total and GAPDH). A nonspecific band can be seen only at the last lane of p-ERK under the low-intensity-specific p-ERK1/2 bands. H) Analysis of proliferation kinetics based on Crystal Violet staining. NIH3T3-CA-NFAT1-ER cells were retrovirally transduced with the specified plasmid (pBabe-Empty or -H-*ras*V12) as described. When indicated, cells were pre-treated with U0126 (20 μM) 2 h prior to stimulation. Cells were treated with OHT (100 nM) when specified and cultured for the specified time. The results are representative of at least 3 independent experiments. US. denotes unstimulated cells in all experiments.

phosphorylation induced by H-*ras*V12 and by PMA stimulation (Fig. 4C), supporting the idea that U0126 inhibition of cell death was occurring through an ERK1/2-dependent pathway. Corroborating these data, another MEK1/2 inhibitor, PD98059, was also able to reduce cell death induced by NFAT1 and H-*ras*12 activation in a dose-response manner (Fig. 4D). Although PD98059 is a selective inhibitor of MEK1/2, it has approximately 100-fold less affinity for MEK1/2 then does U0126 [44]. This could explain the lower level of cell death inhibition (30%) by PD98059 when compared to U0126 (90%; Fig. 4B and D).

To exclude the possibility that H-*ras*V12 could be cooperating with NFAT1 through pathways other than Raf/MEK, and to circumvent any possible nonspecificity of the drugs U0126 and PD98059, we used a constitutively active MEK1 protein (MEK1^{DD}) [35]. Transduction of NIH3T3-CA-NFAT1-ER cells with the plasmid encoding MEK1^{DD} led to the phosphorylation of ERK1/2 at the same level as observed following H-*ras*V12 overexpression (Fig. 4E). Furthermore, MEK1^{DD} expression was sufficient to bypass the need for H-*ras*V12 expression or PMA in the induction of cell death led by NFAT1 (Fig. 4F). Cells expressing CA-NFAT1-ER and MEK1^{DD} underwent cell death at levels comparable to those in cells expressing H-*ras*V12, solely in response to the activation of NFAT1 by OHT. PMA stimulation did not increase the cell death induced by NFAT1 activation and MEK1^{DD} expression, suggesting that the PMA-activated-pathway that cooperates with NFAT1 is, in fact, the Ras/Raf/MEK/ERK pathway (Fig. 4F). To exclude other possible roles of PMA-activated pathways in the induction of cell death, CA-NFAT1-ER-expressing cells were treated with PMA and OHT, and the MEK/ERK pathway was inhibited using U0126 (Fig. 4G). As shown previously, the activation of NFAT1 by OHT and stimulation by PMA strongly induced cell death. However, the inhibition of the ERK1/2 pathway completely blocked cell death in these cells (Fig. 4G).

Finally, we have previously shown that H-*ras*V12 expression in NIH3T3 cells is capable of inducing all the hallmarks of cell transformation including loss of contact-induced growth inhibition [16,45]. To visualize the transformation phenotype induced by H-*ras*V12, NIH3T3-CA-NFAT1-ER cells were infected with the plasmid encoding this oncogene or with an empty vector, and the proliferation kinetics were examined (Fig. 4H). Unlike control cells, which stopped growing once they reached confluence, the H-*ras*V12-expressing cells overgrew the monolayer and continued to proliferate beyond confluence. However, activation of NFAT1 by treatment with OHT in cells expressing CA-NFAT1-ER and H-*ras*V12 led to a complete repression of cell accumulation, which resulted in a large decrease in cell numbers (Fig. 4H). Surprisingly, unlike H-*ras*V12-expressing cells treated with the inhibitor U0126, which only displayed a small reduction in their cell proliferation profile, the MEK1/2 inhibitor apparently partially blocked the induction of cell death by NFAT1. However, these cells did not overgrow the monolayer and reached the level of cells expressing H-*ras*V12 in the absent of NFAT1 activation, as one might expect. This might be explained by two possible reasons: first, that the inhibitor U0126 might not completely block cell death induced by NFAT1 and H-*ras*V12, which is in agreement with Fig. 4B, where it inhibits only around 90% of cell death; or second, that NFAT1 signaling independent of MEK1/2 cooperation might influence cell proliferation (e.g. cell cycle entry) in confluent cell culture, inhibiting the monolayer overgrowth. In fact, we have previously shown that NFAT1 expression can induce cell cycle arrest in cultures [16]. However further experiments are needed to investigate this phenomenon. Altogether, these results demonstrate the need for an active Ras/Raf/MEK/ERK pathway for cooperation with the induction of cell death by NFAT1.

3.3. NFAT1 induces an apoptotic cell death phenotype that can be shifted to programmed-necrosis-like cell death by caspase inhibitors

NFAT1 activation clearly induces DNA fragmentation and the accumulation of a Sub-G_0 DNA content, which is an indicative of cells undergoing apoptosis. We next asked whether NFAT1 could induce other phenotype characteristic of cells undergoing cell death by apoptosis. When NFAT1 was activated (OHT) in NIH3T3 cells in the presence of PMA, we observed increased phosphatidylserine exposition compared to controls, as analyzed by annexin V staining (Fig. 5A). The increase of annexin V positive cells was followed by cell permeabilization, as shown by 7-AAD incorporation, which is an indicative of cells undergoing apoptosis followed by late necrosis cell membrane destabilization (Fig. 5A). To further analyze whether NFAT protein can induce apoptosis in NIH3T3 cells, caspase-3 activity was accessed. NFAT1 activation in cooperation with the Ras pathway led to a seven-fold induction of caspase-3 activity, which could be completely blocked by caspase-3 inhibitor, DEVD-fmk (Fig. 5B). A representative spectrum of the caspase-3 assay is shown for better visualization (Fig. 5C). Next, we examined the morphological characteristics of NIH3T3 cells dying under NFAT1 regulation. Accordingly, NIH3T3-CA-NFAT1-ER cells were treated with PMA alone or in the presence of OHT, and cellular morphology was visualized via phase contrast microscopy, while nuclear size and DNA condensation were analyzed by fluorescence microscopy of DAPI-stained DNA. Whereas cells treated with PMA alone displayed a normal fibroblastic appearance, made cell–cell contact and exhibited a normal nuclear size and no pyknotic nuclei, cells with activated NFAT1 were released from cell–cell contacts, had suffered cell shrinkage and exhibited the formation of pyknotic nuclei at 48 h (Arrows, Fig. 5D). These phenotypes increased at 72 h, when more cells displayed these characteristics when NFAT1 was activated, as represented by the formation of pyknotic nuclei observed at a lower magnification (Wide view; Fig. 5D).

To further investigate the apoptotic cell death induced by NFAT1, we checked whether the pan-caspase inhibitor ZVAD-fmk could abolish the cell death induced by this factor. For this purpose, NIH3T3-CA-NFAT1-ER cells were treated with OHT to activate NFAT1 and with PMA when indicated, and cell death was analyzed based on a Sub-G_0 DNA profile and propidium iodide staining in permeable cells. As expected, only a very small number of cells had undergone DNA fragmentation 24 h after stimulation with OHT and PMA in the presence or absence of ZVAD-fmk (Fig. 5E; left panel). Furthermore, ZVAD-fmk alone or in single combination with OHT or PMA did not induce significant cell death, demonstrating that this caspase inhibitor is not by itself responsible for the induction of cell death (Fig. 5E). However, surprisingly, approximately 90% of the cells treated with OHT and PMA in the presence of ZVAD-fmk were permeable at 24 h, as shown by propidium iodide staining (Fig, 5E; right panel). The incorporation of propidium iodide was not through passive incorporation and reflected cell death since control cells did not stain for PI and all cells from ZVAD-fmk treated wells in the presence of OHT and PMA were loose and did not re-adhere to plate after treatment removal (data not shown). Because almost all of the cells treated with OHT and PMA had died in the presence of ZVAD-fmk at 24 h but lacked DNA fragmentation, we assumed that this outcome might not be due to apoptosis but ZVAD-fmk might have shifted to another cell death modality as programmed necrosis. One of the best-studied and fundamental biochemical pathways involved in programmed necrosis is regulated by RIP1 kinase, and the inhibition of this kinase by necrostatin-1 can block this cell death modality [46]. As shown in Fig. 5E, the addition of necrostatin-1 completely blocked cell death induced by OHT and PMA in the presence of ZVAD-fmk, supporting the idea that NFAT1 can induce apoptotic cell death which can be shifted most likely to programmed necrosis by caspase inhibitors (Fig. 5E; right panel).

3.4. TNF-α expression regulated by NFAT1 and the Ras/MAPK pathway is responsible for the induction of cell death

To determine which gene involved in cell death regulation is being induced by NFAT1 in cooperation with the Ras/MAPK pathway, we performed a screening of apoptosis-related genes using a real-time PCR assay (RT^2 Profiler PCR array). mRNA from NIH3T3-CA-NFAT1-ER-expressing cells was isolated 24 h after stimulation with PMA alone or in the presence of OHT, since 24 h is the NFAT1 transactivation peak and there is no apparent cell death at that time. NFAT1 activation, in cooperation with PMA, led to a 5656-fold up-regulation of TNF-α mRNA levels and more discrete increases in TRAF-1 (223 fold), TRAIL (47 fold), Pak-7 (25 fold) and Fas receptor (7 fold) (Fig. 6A). The expression of the other 79 genes showed changes of less than 2 fold, which is a good indication that the experiment was conducted correctly and that NFAT1 actually only regulates the mentioned genes in this model. Because TNF-α was the most up-regulated gene and is a direct inducer of cell death through apoptosis, we next analyzed protein production for this cytokine. NIH3T3-CA-NFAT1-ER-expressing cells were stimulated by OHT and/or PMA or left unstimulated, and TNF-α accumulation was analyzed by ELISA (Fig. 6B). While stimulation with OHT or PMA alone did not induce TNF-α production at any time point checked, activation of NFAT1 and the Ras/MAPK pathway by PMA led to the accumulation of TNF-α at 24 h after stimulation, with a production peak at 48 h (Fig. 6B), which correlates with the cell death data shown above. TNF-α production is completely dependent on the activation of both NFAT1 and the Ras/Raf/MEK/ERK pathway as demonstrated in Fig. 6C. While TNF-α production induced by NFAT1 (OHT) was completely dependent on the PMA activated pathway, it could be recapitulated by H-*ras*V12 or $MEK1^{DD}$ but not by Empty Vector expression (Fig. 6C), suggesting that Ras/Raf/MEK/ERK pathway is sufficient to cooperate with NFAT1 to the production of TNF-α. Furthermore, the inhibition of MEK1/2 by U0126 completely abolished TNF-α production induced by NFAT1 in cooperation with PMA or H-*ras*V12,

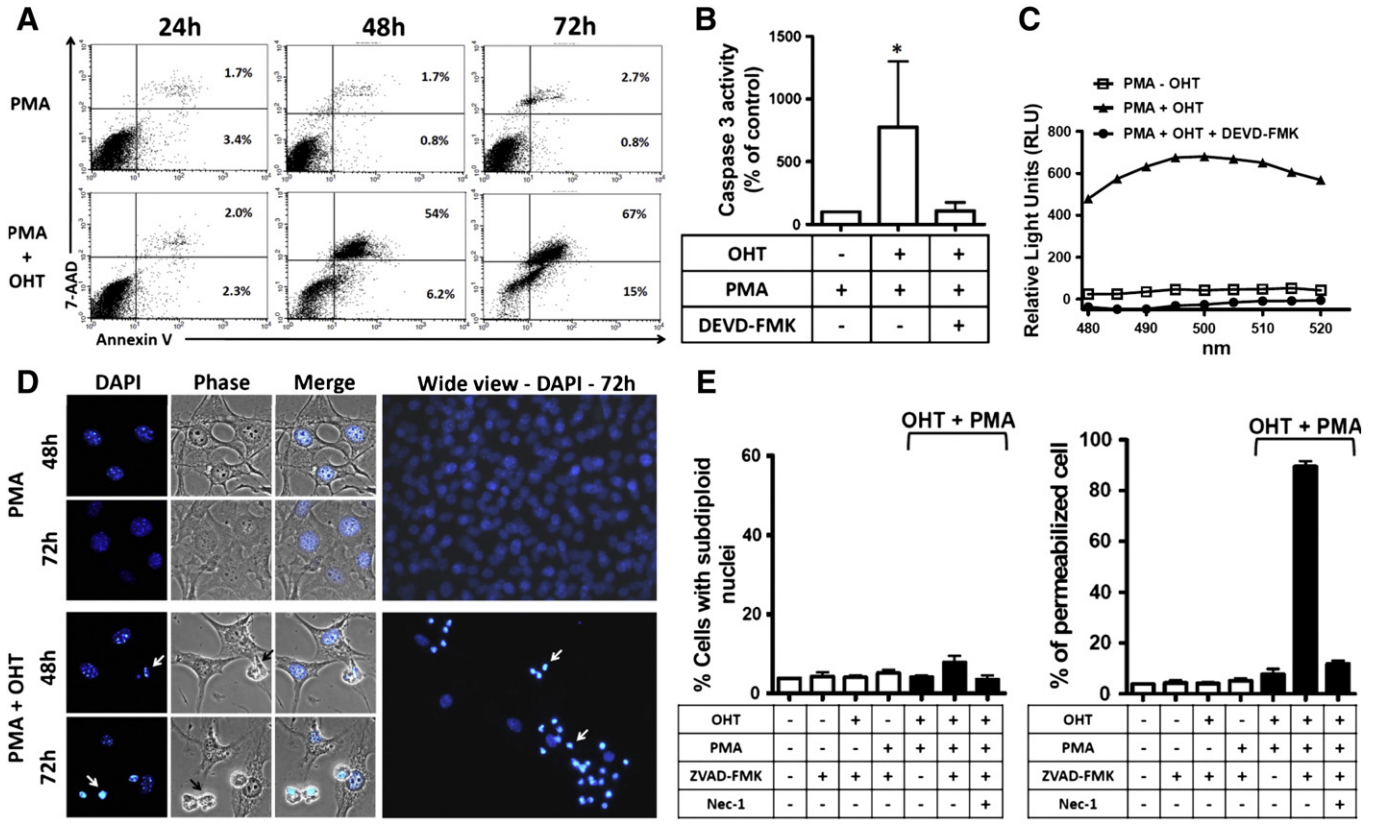

Fig. 5. NFAT1 induces an apoptotic cell death phenotype that can be shifted to programmed-necrosis-like cell death by caspase inhibitors. NIH3T3-CA-NFAT1-ER cells were used for all experiments. A) Apoptotic cell death accompanied by phosphatidylserine exposition. Cells were plated and treated with PMA (20 nM) and OHT (100 nM) when indicated. At the specified time, cells were harvested and stained with Annexin-V and 7-AAD. Cells were analyzed via flow cytometry to detect phosphatidylserine exposition and cell permeabilization. B and C) Caspase-3 activity assay. Cells were plated, treated with PMA (20 nM) and OHT (100 nM) when indicated and harvested 48 h later. Caspase-3 activity was assessed, and as a control, the caspase-3 inhibitor DEVD-FMK was used as described. The fluorescence of cell extracts was analyzed with excitation at 400 nm and emission at 505 nm (B) or by excitation at 400 nm and with a screening emission of 480 to 520 nm (C). B) Caspase-3 activity was normalized and expressed as a % relative to cells treated only with PMA. SD values indicate the variance of at least three independent experiments, and (*) indicates $p \leq 0.001$. C) Representative spectrum from (B). D) Analysis of the formation of pyknotic nuclei and cell morphology. Cells were plated and treated 24 h later with OHT (100 nM) and PMA (20 nM) as indicated. At the specified time, cells were stained with DAPI and analyzed by fluorescence or phase contrast microscopy. Cells undergoing the formation of pyknotic nuclei (white arrows) and displaying apoptotic morphology (black arrows) are indicated. E) Cell death analysis based on the formation of subdiploid nuclei (Sub-G_0; left panel) and cell permeabilization (right panel). Cells were pre-treated when indicated with 20 μM Pan caspase inhibitor (ZVAD-FMK) and 20 μM necrostatin-1 (Nec1) for 2 h prior to treatment with OHT (100 nM) and PMA (20 nM) and cultured for 24 h. Cells were then stained with PI and analyzed by flow cytometry for DNA content and cell permeabilization, as described. SD values indicate the variance of at least three independent experiments.

suggesting that the Ras/Raf/MEK/ERK pathway is necessary to cooperate with NFAT1 for the production of TNF-α. To investigate whether TNF-α is directly implicated in cell death induction in NIH3T3 cells, we stimulated these cells with OHT and PMA and tested whether TNF-α neutralization could prevent cell death. While control cells underwent cell death as expected, pre-treatment of these cells with the neutralizing TNF-α antibody reduced cell death in a dose-response manner, with the maximum reduction reaching approximately 80% (Fig. 6D). These data support a direct involvement of TNF-α accumulation in the induction of cell death in NIH3T3 cells. However, since TNF-α, when bound to its receptor, TNFR1, can activate three main pathways, an inflammatory, an apoptotic or a necrotic pathway, we next evaluated whether TNF-α was directly and solely responsible for the phenotypes induced by NFAT1. To examine whether TNF-α is capable to induce cell death by apoptosis, NIH3T3 *wild type* cells were treated with recombinant mouse TNF-α to obtain a concentration-response curve (Fig. 6E). TNF-α addition led to an induction of the cell death in a concentration-dependent manner leading to massive subdiploid nuclei formation accompanied by cell permeabilization at 72 h (Fig. 6E). Furthermore, the addition of recombinant TNF-α to NIH3T3 cells completely recapitulated the cell death phenotype induced by NFAT1 and PMA in the presence of pan-caspase inhibitor, ZVAD-fmk (Figs. 5E and 6F). While TNF-α or ZVAD-fmk alone did not induce significant cell death at an early time point (24 h) when evaluated by subdiploid nuclei formation or by cell permeabilization (Fig. 6F), they promptly induced cell death in combination (TNF-α plus ZVAD-fmk; Fig. 6F). Cells treated with TNF-α and ZVAD-fmk displayed high level of cell permeabilization but no significant level of cells with DNA fragmentation, an indicative of cells undergoing programmed necrosis (Fig. 6F). Corroborating these data, the process of cell death was almost completely blocked by necrostatin-1 (Fig. 6F, right panel). These data support a mechanism where TNF-α can activate a primary apoptotic pathway in NIH3T3 cells that can be shifted to a programmed necrotic pathway when caspases are blocked. Altogether, these data support the idea that NFAT1 activation, in cooperation with the Ras/Raf/MEK/ERK pathway, is able to induce TNF-α production and accumulation, and that this phenomenon is directly implicated in the induction of cell death in NIH3T3 cells.

4. Discussion

Although the function of NFAT proteins is better characterized in the regulation of the immune response, recent works have postulated

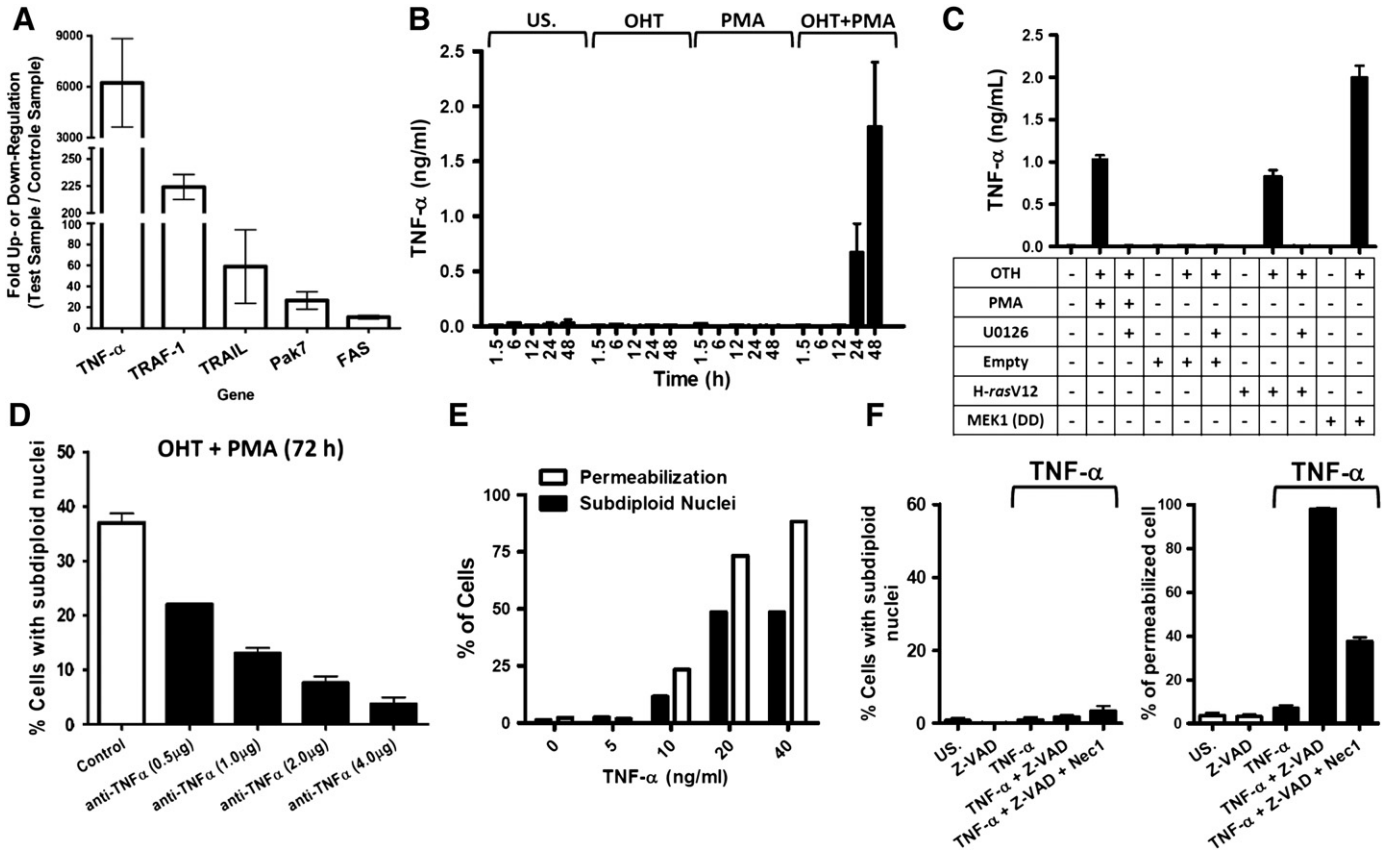

Fig. 6. NFAT1 induces cell death through up-regulation of TNF-α expression in cooperation with the Ras/Raf/MEK/ERK pathway. NIH3T3-CA-NFAT1-ER-expressing cells were used for all experiments. A) SuperArray analysis of gene expression regulated by NFAT1. Cells were plated and treated with PMA (20 nM) alone (Control Sample) or PMA (20 nM) with OHT (100 nM) (Test Sample). After 24 h, mRNA was extracted and used for real-time SuperArray analysis, as described. The fold change values are relative to the Control Sample. Bars indicate the range of two independent experiments. B and C) Analysis of TNF-α protein levels. NIH3T3-CA-NFAT1-ER cells non-transduced (B) or transduced with Empty-, H-*ras*V12- or MEK1^{DD}-expressing vectors (C) were plated and treated with OHT (100 nM) and PMA (20 nM) as indicated, and the cell-free supernatant was assessed for TNF-α protein levels by ELISA at the indicated time, as described, or at 48 h in Figure C. When indicated, cells were pre-treated with U0126 (20 μM) 2 h prior to stimulation. US. denotes unstimulated cells. D and E) Cell death analyzed based on the formation of subdiploid nuclei (Sub-G_0). D) NIH3T3-CA-NFAT1-ER cells were pre-treated when indicated with variable amounts of a TNF-α neutralizing antibody (anti-TNF-α) for 2 h prior to treatment with OHT (100 nM) and PMA (20 nM) and cultured for 72 h. Cells were stained with PI and analyzed by flow cytometry to determine their DNA content at the specified time. E) NIH3T3 *wild type* cells were treated with variable amounts recombinant murine TNF-α and cultured for 72 h. Cells were stained with PI and analyzed by flow cytometry to determine their DNA content and cell permeabilization. F) Cell death analysis based on the formation of subdiploid nuclei (Fig. 6F, left panel) and cell permeabilization (Fig. 6F, right panel). Cells were pre-treated when indicated with 20 μM Pan caspase inhibitor (ZVAD-FMK) and 20 μM necrostatin-1 (Nec1) for 2 h prior to treatment with recombinant murine TNF-α (20 ng) and cultured for 24 h. Cells were then stained with PI and analyzed by flow cytometry for DNA content and cell permeabilization, as described. B, C, D, E and F) SD values indicate the variance of at least three independent experiments.

a major involvement of this family of transcription factors in tumor development and progression [4]. We, and others, have previously proposed that NFAT1 can function as a tumor suppressor gene, possibly through the induction of cell death in transformed cells [15,16]. However, the mechanism by which NFAT1 might exert this role is still elusive. Here, we have shown that NFAT1 protein can induce cell death in NIH3T3 fibroblasts, in cooperation with the oncogenic H-*ras* pathway (Figs. 2 and 3). It has been demonstrated that NFκB can cooperate with NFAT in the induction of cell death in aggressive B-cell lymphomas through the induction of B-lymphocyte stimulator (BLyS) [47]. Despite the activation of NFκB by PMA, this pathway was not found to cooperate in the induction of cell death by NFAT1 (Fig. 3). Furthermore, we determined that the activation of the Ras/Raf/MEK/ERK1/2 pathway is fundamental for the induction of cell death by NFAT1, whereas JNK and p38 MAPK activation is dispensable (Fig. 4). NFAT1 can induce a mixed mode of cell death consisting predominately of apoptotic phenotype cell death that can be shifted for a programmed necrotic cell death pathway in the presence of caspase inhibitors (Fig. 5). Finally, NFAT1, in cooperation with the H-*ras* pathway, induces cell death through the up-regulation of TNF-α gene and protein production, which can be almost completely abolished by neutralization of TNF-α (Fig. 6). These data support the idea that cooperation between NFAT1 and the Ras/Raf/MEK/ERK pathway is involved in the induction of cell death through TNF-α production and possibly in tumor suppression initiated by this transcription factor.

The Ras/Raf/MEK/ERK pathway is most often associated with the induction of cell transformation and tumor progression, being activated in over 90% of pancreatic cancers, 66% of all melanomas and 50% of most types of carcinoma [48]. Activated ERK1/2 phosphorylates and regulates the activities of an ever growing roster of substrates that are estimated to compromise over 160 proteins, including several kinases, phosphatases, transcription factors and cytoskeletal proteins [49]. Furthermore, depending on the particular cell type involved, ERK signaling can regulate processes involved in cell transformation, such as proliferation, differentiation, survival, migration, angiogenesis and chromatin remodeling [48]. However, recent works have postulated that ERK signaling can also induce the cell death machinery directly via the up-regulation of the pro-apoptotic proteins Bax and p53, or indirectly by sensitizing tumor cells through the up-regulation of TRAIL death receptor 4 [50–53]. These data support a dual role for ERK signaling, which might exert a pro- or anti-tumorigenic effect depending on the presence of other still not well-characterized pathways. Our data support the idea

that the NFAT1 pathway can cooperate with ERK1/2 signaling in the induction of cell death and, thus, in accord with our previously published data, possibly cooperate in the induction of a tumor suppression phenotype [16].

Apoptosis operates in adult organisms to maintain normal cellular homeostasis. Violation of this cellular process can result in cancer, autoimmunity, and other diseases. The apoptotic pathway is morphologically characterized by rounding-up of cells, reduction of the cellular volume, and chromatin condensation and fragmentation, while biochemically, it involves caspase activation, culminating in caspase-3 activation, and exposition of phosphatidylserine [54]. As demonstrated here, NFAT1 can induce all of these characteristics in NIH3T3 fibroblasts. It was previously proposed that NFAT proteins can induce apoptosis in different models and cell types, such as in T-lymphocytes, fibroblasts, and neurons, though the mechanism underlying this function is still controversial [16,17,55,56]. NFAT1 is highly expressed in peripheral T cells involved in controlling the termination of the immune response by inducing apoptosis. Activation-induced cell death (AICD) is a particular form of apoptosis that is important for the maintenance of immune system homeostasis. One important route of AICD is the activation of so-called death receptors by their ligands, particularly, FasL, TNF-α, and, more recently, TRAIL. Here, we show that in coordination with ERK1/2 signaling, NFAT1 proteins can robustly up-regulate TNF-α gene expression and, more discretely, that of the TRAIL gene, whereas no effect on FasL expression was detected, in NIH3T3 cells. Moreover, TNF-α protein expression was associated with at least 80% of the total cell death observed, supporting a key role for this cytokine in the induction of apoptosis in this model. NFAT1 activation also led to the up-regulation of other genes involved in cell death, such as TRAF-1 and the FAS receptor (Fig. 6A). Although transcriptional regulation of TRAF-1 by NFAT1 has not been described, this up-regulation could represent indirect regulation via NFκB activation through the ligation of TNF-α to its receptor [57]. Furthermore, although the up-regulation of the FAS receptor through NFAT1 activation could be involved in the induction of cell death in NIH3T3 cells, there was no significant detection of FasL mRNA that could explain this phenomenon (data not shown). NFAT1 was apparently able to induce different cell death pathways consisting mainly of apoptosis but with a contribution of programmed necrotic cell death in the presence of inhibited caspases. Recent pharmacological and genetic evidence suggests that necrosis can occur in a tightly regulated fashion and mediate programmed cell death, in which signaling through RIP1 kinase appears to be essential [58]. Although this hypothesis is still controversial, programmed necrosis might have large implications in cancer development and, possibly, treatment because several cancer cell lines are sensitive to this death modality when treated with DNA damaging compounds or with death receptor ligands, such as TRAIL and TNF-α [59]. Programmed necrosis generally only occurs in cells where the apoptotic protein caspase-8 is inhibited by a caspase inhibitor, such as Z-VAD-fmk, or in cells that overexpress the caspase-8 inhibitor FLICE-inhibitory protein short isoform (FLIPs) [60]. Our data clearly show that NFAT1 can induce cell death through programmed necrosis in the presence of Z-VAD-fmk, as characterized by the observation of cell permeabilization without nuclear fragmentation and by the dependency of the activity of RIP1 kinase, as shown using its inhibitor necrostatin-1 (Fig. 5E). In vivo, the inhibition of programmed necrosis by necrostatin-1 was shown to delay ischemic brain injury in mice, inhibit myocardial cell death, and reduce infarct size [61]. One interesting correlation is that TNF-α is one of the main molecules involved in this pathology and that NFAT1 protein is expressed in both the brain and myocardial cells. Altogether, these data support a possible mechanism through which NFAT1 could regulate the induction of cell death via apoptosis and, in the presence of inhibited caspases as in cells that overexpress FLICE protein, could induce programmed necrosis, contributing to further understanding the involvement of this transcription factor in cancer, immune response termination and, possibly, brain and heart injuries.

The regulation of TNF-α expression by NFAT1 could account for both the apoptotic and the programmed necrotic cell death observed in NIH3T3 cells. Ligation of TNF-α to its receptor, TNFR1, can activate three main pathways: (1) NFκB, leading to a pro-inflammatory and anti-apoptotic response; (2) caspases, leading to apoptosis; and (3) RIP1 and RIP3, in the absence of caspase-8 activity, which leads to necrotic cell death [61]. TNF-α transcription can be activated in the immune system by a diverse group of well-described stimuli depending on the cell type involved, such as through toll-like receptor activation (TLR), T- and B-cell receptor antigen ligation, and stimulation by cytokines such as IL-1, IFN-γ and TNF-α itself [62]. The TNF-α proximal promoter displays a highly conserved region of approximately 200 nucleotides in mammals that contains biding motifs that can be recognized by transcription factors activated downstream of these stimuli [62]. Six NFAT binding sites have been identified in the TNF-α promoter, in addition to four Ets/Elk, two Sp1, and one ATF-2/c-Jun binding sites [62–64]. It has previously been demonstrated that NFAT signaling can cooperate with downstream pathways activated by JNK and p38 kinases in the transactivation of the TNF-α gene, possibly through the activation of and cooperation with the ATF-2 and c-Jun transcription factors [65–67]. Here, we have shown that in H-*ras*V12-transformed fibroblasts, both the NFAT1 and ERK1/2 signaling pathways are fundamental for the transcriptional up-regulation of the TNF-α gene, while JNK and p38 signaling are dispensable. Mechanistically, ERK1/2 kinases could augment the DNA binding activity of NFAT directly by phosphorylating its N- and C-termini, which would culminate in increased binding of NFAT to the TNF-α promoter and, thus, increased expression [68]. However, ERK1/2 signaling can also activate the Elk-1, SP-1, ATF-2 and c-Jun transcription factors, which could bind to the TNF-α promoter and cooperate with NFAT1 to induce TNF-α expression [49]. Although our data clearly show cooperation between NFAT1 and ERK1/2 in TNF-α gene regulation, further experiments are needed to specify which signal downstream of ERK is responsible for this phenomenon.

While the major obstacle to the therapeutic exploitation of TNF-α for cancer treatment is its ability to elicit a systemic inflammatory response syndrome, the expression of NFAT1 proteins in tumors exhibiting an activated Ras/Raf/MEK/ERK pathway could lead to massive local production of TNF-α and, thus, induce tumor suppression with a lower systemic inflammatory effect. Furthermore, the Ras/Raf/MEK/ERK oncogenic pathway might sensitize transformed cells to NFAT1-induced cell death, and thus, NFAT1 could convert a well-characterized oncogenic pathway to become a tumor suppressor pathway. NFAT1 overexpression could be a potential mechanism to be exploited in gene therapy for cancers that exhibit the over-activation of the MEK/ERK pathway, leading to more-specific, targeted treatment.

Acknowledgements

We are especially grateful to Dr. A. Rao for kindly providing the NFAT reagents and to Dr. B.L. Diaz for providing the MAPK reagents. We are grateful to M.A. Rajão for confocal microscope technical support, Dr. G. Evan for the pBabe-c-mycER™ plasmid, Dr. S. Lowe for the pBabe-H-rasV12 and pBabe-IκBα-mut plasmids, and Dr. W. Hahn for the pBabe-MEK1^{DD} plasmid. This work was supported by grants to J.P.B.V. from the ICGEB (CRP/BRA09-01), CNPq (478780/2010-9), FAPERJ (102.357/2009) and INCT-Cancer (573806/2008-0 and 170.026/2008). B.K.R. was supported by a CAPES fellowship and P.I.L. was supported by a Brazilian Ministry of Health fellowship.

References

[1] A. Rao, C. Luo, P.G. Hogan, Transcription factors of the NFAT family: regulation and function, Annu. Rev. Immunol. 15 (1997) 707–747.
[2] F. Macian, NFAT proteins: key regulators of T-cell development and function, Nat. Rev. Immunol. 5 (2005) 472–484.
[3] I.A. Graef, F. Chen, G.R. Crabtree, NFAT signaling in vertebrate development, Curr. Opin. Genet. Dev. 11 (2001) 505–512.

[4] M. Mancini, A. Toker, NFAT proteins: emerging roles in cancer progression, Nat. Rev. Cancer 9 (2009) 810–820.
[5] N.A. Clipstone, G.R. Crabtree, Identification of calcineurin as a key signalling enzyme in T-lymphocyte activation, Nature 357 (1992) 695–697.
[6] J. Park, N.R. Yaseen, P.G. Hogan, A. Rao, S. Sharma, Phosphorylation of the transcription factor NFATp inhibits its DNA binding activity in cyclosporin A-treated human B and T cells, J. Biol. Chem. 270 (1995) 20653–20659.
[7] J. Jain, C. Loh, A. Rao, Transcriptional regulation of the IL-2 gene, Curr. Opin. Immunol. 7 (1995) 333–342.
[8] H.D. Youn, T.A. Chatila, J.O. Liu, Integration of calcineurin and MEF2 signals by the coactivator p300 during T-cell apoptosis, EMBO J. 19 (2000) 4323–4331.
[9] J.P. Viola, L.D. Carvalho, B.P. Fonseca, L.K. Teixeira, NFAT transcription factors: from cell cycle to tumor development, Braz. J. Med. Biol. Res. 38 (2005) 335–344.
[10] G.P. Mognol, P.S. de Araujo-Souza, B.K. Robbs, L.K. Teixeira, J.P. Viola, Transcriptional regulation of the c-Myc promoter by NFAT1 involves negative and positive NFAT-responsive elements, Cell Cycle 11 (2012) 1014–1028.
[11] M.R. Hodge, A.M. Ranger, F. Charles de la Brousse, T. Hoey, M.J. Grusby, L.H. Glimcher, Hyperproliferation and dysregulation of IL-4 expression in NF-ATp-deficient mice, Immunity 4 (1996) 397–405.
[12] S. Xanthoudakis, J.P. Viola, K.T. Shaw, C. Luo, J.D. Wallace, P.T. Bozza, D.C. Luk, T. Curran, A. Rao, An enhanced immune response in mice lacking the transcription factor NFAT1, Science 272 (1996) 892–895.
[13] K. Schuh, B. Kneitz, J. Heyer, U. Bommhardt, E. Jankevics, F. Berberich-Siebelt, K. Pfeffer, H.K. Muller-Hermelink, A. Schimpl, E. Serfling, Retarded thymic involution and massive germinal center formation in NF-ATp-deficient mice, Eur. J. Immunol. 28 (1998) 2456–2466.
[14] M.S. Caetano, A. Vieira-de-Abreu, L.K. Teixeira, M.B. Werneck, M.A. Barcinski, J.P. Viola, NFATC2 transcription factor regulates cell cycle progression during lymphocyte activation: evidence of its involvement in the control of cyclin gene expression, FASEB J. 16 (2002) 1940–1942.
[15] A.M. Ranger, L.C. Gerstenfeld, J. Wang, T. Kon, H. Bae, E.M. Gravallese, M.J. Glimcher, L.H. Glimcher, The nuclear factor of activated T cells (NFAT) transcription factor NFATp (NFATc2) is a repressor of chondrogenesis, J. Exp. Med. 191 (2000) 9–22.
[16] B.K. Robbs, A.L. Cruz, M.B. Werneck, G.P. Mognol, J.P. Viola, Dual roles for NFAT transcription factor genes as oncogenes and tumor suppressors, Mol. Cell. Biol. 28 (2008) 7168–7181.
[17] S. Chuvpilo, E. Jankevics, D. Tyrsin, A. Akimzhanov, D. Moroz, M.K. Jha, J. Schulze-Luehrmann, B. Santner-Nanan, E. Feoktistova, T. Konig, A. Avots, E. Schmitt, F. Berberich-Siebelt, A. Schimpl, E. Serfling, Autoregulation of NFATc1/A expression facilitates effector T cells to escape from rapid apoptosis, Immunity 16 (2002) 881–895.
[18] E. Kondo, A. Harashima, T. Takabatake, H. Takahashi, Y. Matsuo, T. Yoshino, K. Orita, T. Akagi, NF-ATc2 induces apoptosis in Burkitt's lymphoma cells through signaling via the B cell antigen receptor, Eur. J. Immunol. 33 (2003) 1–11.
[19] A.M. Pedrosa, R. Weinlich, G.P. Mognol, B.K. Robbs, J.P. Viola, A. Campa, G.P. Amarante-Mendes, Melatonin protects CD4+ T cells from activation-induced cell death by blocking NFAT-mediated CD95 ligand upregulation, J. Immunol. 184 (2010) 3487–3494.
[20] D.V. Faget, P.I. Lucena, B.K. Robbs, J.P. Viola, NFAT1 C-terminal domains are necessary but not sufficient for inducing cell death, PLoS One 7 (2012).
[21] W.L. Blalock, C. Weinstein-Oppenheimer, F. Chang, P.E. Hoyle, X.Y. Wang, P.A. Algate, R.A. Franklin, S.M. Oberhaus, L.S. Steelman, J.A. McCubrey, Signal transduction, cell cycle regulatory, and anti-apoptotic pathways regulated by IL-3 in hematopoietic cells: possible sites for intervention with anti-neoplastic drugs, Leukemia 13 (1999) 1109–1166.
[22] J.A. McCubrey, L.S. Steelman, W.H. Chappell, S.L. Abrams, E.W. Wong, F. Chang, B. Lehmann, D.M. Terrian, M. Milella, A. Tafuri, F. Stivala, M. Libra, J. Basecke, C. Evangelisti, A.M. Martelli, R.A. Franklin, Roles of the Raf/MEK/ERK pathway in cell growth, malignant transformation and drug resistance, Biochim. Biophys. Acta 1773 (2007) 1263–1284.
[23] L.S. Steelman, S.C. Pohnert, J.G. Shelton, R.A. Franklin, F.E. Bertrand, J.A. McCubrey, JAK/STAT, Raf/MEK/ERK, PI3K/Akt and BCR-ABL in cell cycle progression and leukemogenesis, Leukemia 18 (2004) 189–218.
[24] H. Rajagopalan, A. Bardelli, C. Lengauer, K.W. Kinzler, B. Vogelstein, V.E. Velculescu, Tumorigenesis: RAF/RAS oncogenes and mismatch-repair status, Nature 418 (2002) 934.
[25] K.E. Mercer, C.A. Pritchard, Raf proteins and cancer: B-Raf is identified as a mutational target, Biochim. Biophys. Acta 1653 (2003) 25–40.
[26] G. Singer, R. Oldt III, Y. Cohen, B.G. Wang, D. Sidransky, R.J. Kurman, M. Shih Ie, Mutations in BRAF and KRAS characterize the development of low-grade ovarian serous carcinoma, J. Natl. Cancer Inst. 95 (2003) 484–486.
[27] M.D. Vos, A. Martinez, C.A. Ellis, T. Vallecorsa, G.J. Clark, The pro-apoptotic Ras effector Nore1 may serve as a Ras-regulated tumor suppressor in the lung, J. Biol. Chem. 278 (2003) 21938–21943.
[28] N.L. Sieben, P. Macropoulos, G.M. Roemen, S.M. Kolkman-Uljee, G. Jan Fleuren, R. Houmadi, T. Diss, B. Warren, M. Al Adnani, A.P. De Goeij, T. Krausz, A.M. Flanagan, In ovarian neoplasms, BRAF, but not KRAS, mutations are restricted to low-grade serous tumours, J. Pathol. 202 (2004) 336–340.
[29] P.J. Roberts, C.J. Der, Targeting the Raf-MEK-ERK mitogen-activated protein kinase cascade for the treatment of cancer, Oncogene 26 (2007) 3291–3310.
[30] C. Loh, J.A. Carew, J. Kim, P.G. Hogan, A. Rao, T-cell receptor stimulation elicits an early phase of activation and a later phase of deactivation of the transcription factor NFAT1, Mol. Cell. Biol. 16 (1996) 3945–3954.
[31] H. Okamura, J. Aramburu, C. Garcia-Rodriguez, J.P. Viola, A. Raghavan, M. Tahiliani, X. Zhang, J. Qin, P.G. Hogan, A. Rao, Concerted dephosphorylation of the transcription factor NFAT1 induces a conformational switch that regulates transcriptional activity, Mol. Cell 6 (2000) 539–550.
[32] L.K. Teixeira, B.P. Fonseca, A. Vieira-de-Abreu, B.A. Barboza, B.K. Robbs, P.T. Bozza, J.P. Viola, IFN-gamma production by CD8+ T cells depends on NFAT1 transcription factor and regulates Th differentiation, J. Immunol. 175 (2005) 5931–5939.
[33] T.D. Littlewood, D.C. Hancock, P.S. Danielian, M.G. Parker, G.I. Evan, A modified oestrogen receptor ligand-binding domain as an improved switch for the regulation of heterologous proteins, Nucleic Acids Res. 23 (1995) 1686–1690.
[34] M. Serrano, A.W. Lin, M.E. McCurrach, D. Beach, S.W. Lowe, Oncogenic ras provokes premature cell senescence associated with accumulation of p53 and p16INK4a, Cell 88 (1997) 593–602.
[35] J.S. Boehm, J.J. Zhao, J. Yao, S.Y. Kim, R. Firestein, I.F. Dunn, S.K. Sjostrom, L.A. Garraway, S. Weremowicz, A.L. Richardson, H. Greulich, C.J. Stewart, L.A. Mulvey, R.R. Shen, L. Ambrogio, T. Hirozane-Kishikawa, D.E. Hill, M. Vidal, M. Meyerson, J.K. Grenier, G. Hinkle, D.E. Root, T.M. Roberts, E.S. Lander, K. Polyak, W.C. Hahn, Integrative genomic approaches identify IKBKE as a breast cancer oncogene, Cell 129 (2007) 1065–1079.
[36] K.E. Hedin, M.P. Bell, K.R. Kalli, C.J. Huntoon, B.M. Sharp, D.J. McKean, Delta-opioid receptors expressed by Jurkat T cells enhance IL-2 secretion by increasing AP-1 complexes and activity of the NF-AT/AP-1-binding promoter element, J. Immunol. 159 (1997) 5431–5440.
[37] H.L. Pahl, P.A. Baeuerle, A novel signal transduction pathway from the endoplasmic reticulum to the nucleus is mediated by transcription factor NF-kappa B, EMBO J. 14 (1995) 2580–2588.
[38] A.J. Shaywitz, M.E. Greenberg, CREB: a stimulus-induced transcription factor activated by a diverse array of extracellular signals, Annu. Rev. Biochem. 68 (1999) 821–861.
[39] T.A. McKinsey, C.L. Zhang, E.N. Olson, MEF2: a calcium-dependent regulator of cell division, differentiation and death, Trends Biochem. Sci. 27 (2002) 40–47.
[40] R.R. Ahangarani, W. Janssens, V. Carlier, L. Vanderelst, T. Vandendriessche, M. Chuah, M. Jacquemin, J.M. Saint-Remy, Retroviral vectors induce epigenetic chromatin modifications and IL-10 production in transduced B cells via activation of toll-like receptor 2, Mol. Ther. 19 (2011) 711–722.
[41] J.P. Roose, M. Mollenauer, V.A. Gupta, J. Stone, A. Weiss, A diacylglycerol-protein kinase C-RasGRP1 pathway directs Ras activation upon antigen receptor stimulation of T cells, Mol. Cell. Biol. 25 (2005) 4426–4441.
[42] B. Ko, L.M. Joshi, L.L. Cooke, N. Vazquez, M.W. Musch, S.C. Hebert, G. Gamba, R.S. Hoover, Phorbol ester stimulation of RasGRP1 regulates the sodium-chloride cotransporter by a PKC-independent pathway, Proc. Natl. Acad. Sci. U. S. A. 104 (2007) 20120–20125.
[43] J.Y. Byun, C.H. Yoon, S. An, I.C. Park, C.M. Kang, M.J. Kim, S.J. Lee, The Rac1/MKK7/JNK pathway signals upregulation of Atg5 and subsequent autophagic cell death in response to oncogenic Ras, Carcinogenesis 30 (2009) 1880–1888.
[44] M.F. Favata, K.Y. Horiuchi, E.J. Manos, A.J. Daulerio, D.A. Stradley, W.S. Feeser, D.E. Van Dyk, W.J. Pitts, R.A. Earl, F. Hobbs, R.A. Copeland, R.L. Magolda, P.A. Scherle, J.M. Trzaskos, Identification of a novel inhibitor of mitogen-activated protein kinase kinase, J. Biol. Chem. 273 (1998) 18623–18632.
[45] D. Hanahan, R.A. Weinberg, Hallmarks of cancer: the next generation, Cell 144 (2011) 646–674.
[46] D. Moquin, F.K. Chan, The molecular regulation of programmed necrotic cell injury, Trends Biochem. Sci. 35 (2010) 434–441.
[47] L. Fu, Y.C. Lin-Lee, L.V. Pham, A. Tamayo, L. Yoshimura, R.J. Ford, Constitutive NF-kappaB and NFAT activation leads to stimulation of the BLyS survival pathway in aggressive B-cell lymphomas, Blood 107 (2006) 4540–4548.
[48] A.S. Dhillon, S. Hagan, O. Rath, W. Kolch, MAP kinase signalling pathways in cancer, Oncogene 26 (2007) 3279–3290.
[49] S. Yoon, R. Seger, The extracellular signal-regulated kinase: multiple substrates regulate diverse cellular functions, Growth Factors 24 (2006) 21–44.
[50] K.G. Drosopoulos, M.L. Roberts, L. Cermak, T. Sasazuki, S. Shirasawa, L. Andera, A. Pintzas, Transformation by oncogenic RAS sensitizes human colon cells to TRAIL-induced apoptosis by up-regulating death receptor 4 and death receptor 5 through a MEK-dependent pathway, J. Biol. Chem. 280 (2005) 22856–22867.
[51] Y.K. Kim, H.J. Kim, C.H. Kwon, J.H. Kim, J.S. Woo, J.S. Jung, J.M. Kim, Role of ERK activation in cisplatin-induced apoptosis in OK renal epithelial cells, J. Appl. Toxicol. 25 (2005) 374–382.
[52] B.G. Park, C.I. Yoo, H.T. Kim, C.H. Kwon, Y.K. Kim, Role of mitogen-activated protein kinases in hydrogen peroxide-induced cell death in osteoblastic cells, Toxicology 215 (2005) 115–125.
[53] D.W. Li, J.P. Liu, Y.W. Mao, H. Xiang, J. Wang, W.Y. Ma, Z. Dong, H.M. Pike, R.E. Brown, J.C. Reed, Calcium-activated RAF/MEK/ERK signaling pathway mediates p53-dependent apoptosis and is abrogated by alpha B-crystallin through inhibition of RAS activation, Mol. Biol. Cell 16 (2005) 4437–4453.
[54] G. Kroemer, L. Galluzzi, P. Vandenabeele, J. Abrams, E.S. Alnemri, E.H. Baehrecke, M.V. Blagosklonny, W.S. El-Deiry, P. Golstein, D.R. Green, M. Hengartner, R.A. Knight, S. Kumar, S.A. Lipton, W. Malorni, G. Nunez, M.E. Peter, J. Tschopp, J. Yuan, M. Piacentini, B. Zhivotovsky, G. Melino, Classification of cell death: recommendations of the Nomenclature Committee on Cell Death 2009, Cell Death Differ. 16 (2009) 3–11.
[55] K. Yao, Y.Y. Cho, H.R. Bergen III, B.J. Madden, B.Y. Choi, W.Y. Ma, A.M. Bode, Z. Dong, Nuclear factor of activated T3 is a negative regulator of Ras-JNK1/2-AP-1 induced cell transformation, Cancer Res. 67 (2007) 8725–8735.
[56] S. Alvarez, A. Blanco, M. Fresno, M.A. Munoz-Fernandez, TNF-alpha contributes to caspase-3 independent apoptosis in neuroblastoma cells: role of NFAT, PLoS One 6 (2011) e16100.

[57] H. Wajant, K. Pfizenmaier, P. Scheurich, Tumor necrosis factor signaling, Cell Death Differ. 10 (2003) 45–65.
[58] D.R. Green, A. Oberst, C.P. Dillon, R. Weinlich, G.S. Salvesen, RIPK-dependent necrosis and its regulation by caspases: a mystery in five acts, Mol. Cell 44 (2011) 9–16.
[59] P. Kreuzaler, C.J. Watson, Killing a cancer: what are the alternatives? Nat. Rev. Cancer 12 (2012) 411–424.
[60] R. Weinlich, C.P. Dillon, D.R. Green, Ripped to death, Trends Cell Biol. 21 (2011) 630–637.
[61] F. Van Herreweghe, N. Festjens, W. Declercq, P. Vandenabeele, Tumor necrosis factor-mediated cell death: to break or to burst, that's the question, Cell. Mol. Life Sci. 67 (2010) 1567–1579.
[62] J.V. Falvo, A.V. Tsytsykova, A.E. Goldfeld, Transcriptional control of the TNF gene, Curr. Dir. Autoimmun. 11 (2010) 27–60.
[63] A.E. Goldfeld, P.G. McCaffrey, J.L. Strominger, A. Rao, Identification of a novel cyclosporin-sensitive element in the human tumor necrosis factor alpha gene promoter, J. Exp. Med. 178 (1993) 1365–1379.
[64] E.Y. Tsai, J. Jain, P.A. Pesavento, A. Rao, A.E. Goldfeld, Tumor necrosis factor alpha gene regulation in activated T cells involves ATF-2/Jun and NFATp, Mol. Cell. Biol. 16 (1996) 459–467.
[65] E.Y. Tsai, J. Yie, D. Thanos, A.E. Goldfeld, Cell-type-specific regulation of the human tumor necrosis factor alpha gene in B cells and T cells by NFATp and ATF-2/JUN, Mol. Cell. Biol. 16 (1996) 5232–5244.
[66] T. Ishizuka, N. Terada, P. Gerwins, E. Hamelmann, A. Oshiba, G.R. Fanger, G.L. Johnson, E.W. Gelfand, Mast cell tumor necrosis factor alpha production is regulated by MEK kinases, Proc. Natl. Acad. Sci. U. S. A. 94 (1997) 6358–6363.
[67] M.C. Lawrence, B. Naziruddin, M.F. Levy, A. Jackson, K. McGlynn, Calcineurin/nuclear factor of activated T cells and MAPK signaling induce TNF-{alpha} gene expression in pancreatic islet endocrine cells, J. Biol. Chem. 286 (2011) 1025–1036.
[68] B. Sanna, O.F. Bueno, Y.S. Dai, B.J. Wilkins, J.D. Molkentin, Direct and indirect interactions between calcineurin-NFAT and MEK1-extracellular signal-regulated kinase 1/2 signaling pathways regulate cardiac gene expression and cellular growth, Mol. Cell. Biol. 25 (2005) 865–878.